Chaotic states of weakly and strongly nonlinear oscillators with quasiperiodic excitation

D. M. Vavriv,[1] V. B. Ryabov,[1,2] S. A. Sharapov,[1] and H. M. Ito[2]
[1]*Institute of Radio Astronomy, 4 Krasnoznamennaya Street, 310002 Kharkov, Ukraine*
[2]*Seismology and Volcanology Research Department, Meteorological Research Institute, Nagamine 1-1, Tsukuba-shi, Ibaraki-ken, 305, Japan*
(Received 13 April 1995)

A comparative study of conditions for chaos onset in Duffing-type weakly and strongly nonlinear oscillators is carried out. Quasiperiodically forced oscillators with combined parametric and external excitation are considered. The concept of induced saddle states is introduced in order to illuminate reasons for chaos arising in weakly nonlinear systems. The conditions for, and the mechanisms of, the transition to chaos are investigated in detail, both analytically and numerically, for the case of weakly nonlinear oscillators. Multistability properties of the oscillators are studied as well. An important application of the theory is the stability analysis of parametric amplifiers.

PACS number(s): 05.45.+b

I. INTRODUCTION

The phenomena of parametric generation, amplification of oscillations, and frequency conversion are distinguishing features of the dynamics in a variety of physical systems. For single-degree-of-freedom oscillators, which are the subject of the present paper, many of these phenomena can be adequately described within the framework of the universal mathematical model, like the equation

$$\ddot{x}+\omega_0^2[1-M\cos(\omega_p t)]x = -(\delta_0+\delta_1 x^2)\dot{x}+\gamma x^3+A\cos(\omega_e t) \quad (1)$$

of an oscillator subjected to combined parametric and external forcing. Here x is a generalized coordinate, $\delta_0>0$ and $\delta_1>0$ are the coefficients of linear and nonlinear damping, γ is the nonlinearity parameter, ω_0 is the natural frequency of the oscillator, and M and A are the amplitudes of parametric and external forcing with incommensurate frequencies ω_p and ω_e. For example, in the case of optical or microwave parametric amplitudes, M and A are proportional, respectively, to the amplitude of a pumping oscillation and that of a signal wave to be amplified. Note that the oscillator (1) can be considered a Duffing type one, due to the limitations imposed on the coefficients $\delta_0>0$ and $\delta_1>0$.

It is well known that parametric amplifiers often demonstrate a high level of noise in the output signal. Moreover, a sudden increase in the noise level may occur unexpectedly under a comparatively small variation of controls. We suppose that one possible reason for such behavior can be provided by the rise of a chaotic instability. Although this idea is not new and chaos in parametric systems has been studied for a long time, the majority of the investigations have focused on strongly nonlinear operation modes, which are not typical in many practical situations. Therefore, the results obtained in the framework of this approach cannot explain high noise level in weakly nonlinear systems. In this work we show that the high output noise in parametric amplifiers may be due to the appearance of chaotic instability in the weakly nonlinear limit. This problem, being of great importance for applications, has hardly been investigated yet.

Let us briefly mention some results obtained so far for Eq. (1). One such case is the harmonically driven Duffing oscillator, whose dynamics have been extensively investigated by many authors, starting from the now classical works in this field [1–4]. It was shown, in particular, that the rise of chaotic motions is associated with the formation of a homoclinic structure in the phase space of the system, due to a transverse intersection of stable and unstable manifolds of hyperbolic periodic orbits. In the presence of dissipation this intersection occurs if some threshold condition in the external force or nonlinearity parameter is met. Usually, there exists an intrinsic relation between the parameters of external force and the degree of nonlinearity that defines the condition of homoclinc structure formation. It is a commonly accepted notion that under small or nonresonant forcing the system evolves in a weakly nonlinear, or regular, regime, which could be made strongly nonlinear, and even chaotic, either by adjusting the parameters of excitation (increasing the amplitude or frequency tuning to the resonant region) or by increasing the parameter controlling the nonlinearity. It thus seems reasonable to assert that the degree of nonlinearity of a given oscillatory regime is defined by the intensity of oscillations resulting from the excitation or the system's intrinsic properties [5] and the system can be treated as a weakly nonlinear one at small amplitudes of motion, being strongly nonlinear if the oscillations are comparatively intense. It is interesting to note in this respect that it is a widely spread opinion that the nonlinearity parameter must be large for chaos to arise in any single-degree-of-freedom dissipation oscillator with external excitation. However, as already mentioned and will be clear below, it is not exactly so.

Notice that, beginning with the above-mentioned pa-

pers and up to now, mainly systems possessing a homoclinic trajectory (or trajectories) to a hyperbolic saddle point(s) in their Hamiltonian limit have been studied. From now on, we will refer to singular points of this type as original saddle points, due to the fact that these unstable hilltop solutions [6] exist in the nonperturbed oscillators, when the dissipation and amplitudes of external and parametric forces vanish. The systems with an original saddle point are amenable to a theoretical treatment by using a global perturbation technique developed by Melnikov [1], which is presumably the main reason why these systems have received such detailed consideration (see Refs [7,8]). This technique was generalized by Wiggins [9] to the case of quasiperiodically forced oscillators. In the problems of this type, the origin of chaos was once again associated with the existence of the original saddle point and the mechanism for chaotic states to appear was stated to be the same as for harmonically forced oscillators, i.e., a strong nonlinearity plus the intersection of manifolds associated with original saddle points.

However, for quasiperiodically forced oscillators, there is another possible way of chaos arising, which is not directly related to the existence of homoclinic orbits in the nonperturbed system and where the large nonlinearity parameter is not required. In this case, the complicated dynamics and the associated chaotic behavior arise due to the occurrence of various resonances that typically lead to the increase in oscillation amplitude under the variation of control parameters defining the external force. Such a possibility was predicted and studied theoretically by several authors in Refs. [10–12] and proved experimentally in Refs. [13,14]. The alternative way of the transition to chaos here is associated with the appearance of saddle orbits in the vicinity of resonances, which result from the action of one of the harmonic components in the external force. We will refer to such kinds of solutions as induced saddle orbits. With the availability of additional components of comparatively low intensity in the external force, normally hyperbolic invariant tori are formed in the phase space instead of induced saddle trajectories. The chaos thus results from the transverse intersection of stable and unstable manifolds of the induced tori under the increase of perturbation. The formation of a homoclinic structure occurs in such a situation at much lower values of the excitation amplitude compared to the case when this structure arises on the basis of an original saddle point. Moreover, it was found in [15] that any degree of nonlinearity, however small, may initiate the formation of chaotic states. The theoretical and experimental study of applications [14–17] has shown that the threshold of chaos onset with respect to the amplitude of external excitation is decreased by several orders of magnitude when the harmonic force is replaced by a quasiperiodic one. The existence of chaotic states in the weakly nonlinear limit implies that the condition of a large nonlinearity parameter for chaos to arise is not always necessary and the influence of chaotic instabilities my have much more profound effect on the dynamics of real system compared to the one that could be anticipated from the traditional way of thinking. On the other hand, there are a lot of typical situations where one can expect to observe chaotic states under weakly nonlinear excitation conditions, including various types of oscillators with a quasiperiodic force [10–16], multimode autonomous and nonautonomous systems [18–20], distributed systems with wave interaction [21], etc. It should be noted that the origin of chaotic dynamics in weakly nonlinear systems is still not known and many of the principal problems concerning the dynamics of oscillators remain to be considered from this point of view.

In this paper we study the transition to chaos in parametrically forced weakly nonlinear oscillators of type (1) in the vicinity of the primary resonance. Actually, this corresponds to the case of a small resonant periodic perturbation of the system just after the onset of the first periodic-doubling bifurcation. A similar problem, but before the onset of period doubling, has recently attracted significant attention [22] in the context of the stability analysis of nonlinear oscillators. It was shown in particular that such a kind of perturbation may either lead to suppression of the period-doubling supercritical instability [22] or induce the bifurcation if tuned in the subcritical region [23]. We investigate here both cases in the situation when the system's period has been already doubled and the parameter values are tuned within a region far beyond the criticality.

For better illustration of the results obtained, we review, in Sec. II, the conditions for the formation of chaotic states in a strongly nonlinear oscillator and then compare them with the chaotic states in the quasilinear limit. When studying the dynamics of weakly nonlinear oscillators, we use the method of averaging. This enables us to specify a particular resonance problem and investigate in detail the properties of induced saddle states. The transition from Eq. (1) to the averaged system is described in Sec. III, along with the discussion of some properties of the averaged equations. In Sec. IV we make use of these equations to determine the conditions of existence for the induced saddle orbits under the parametric excitation. It should be mentioned that induced saddle trajectories in the initial equation (1) manifest themselves as singular saddle points in the averaged equations.

In the following sections, we focus on the conditions of chaos onset in the weakly nonlinear system. Two typical problems are considered, depending on the number of the induced saddle states coexisting in the phase space and corresponding to super- and subcritical transitions to period-doubled motion in the harmonically excited system [22–24]. Accordingly, Sec. V deals with induced homoclinic orbits, whereas the case with heteroclinic orbits is studied in Sec. VI. In these sections we apply Melnikov's method to the averaged equations in order to obtain analytical conditions for the formation of homoclinic (or heteroclinic) structures associated with the induced saddle states. These results are compared with those deduced from detailed numerical simulations. Characteristic features of the oscillators' dynamics pertaining to the rise of chaotic and multistable states are also considered. Finally, Sec. VII contains a summary and discussion. Some additional information on the dynamics of weakly nonlinear oscillators with parametric excitation can be found in Refs. [12,16,25–29].

II. STRONGLY NONLINEAR OSCILLATORS

In this section we review some general conditions for the rise of chaotic states in the strongly nonlinear oscillators. Let us rewrite Eq. (1) as a system of first-order equations

$$\dot{x}=y\ ,\quad \dot{y}=-\omega_0^2 x+\varepsilon f(x,y,t)\ , \tag{2}$$

where

$$f(x,y,t)=-(\delta_0+\delta_1 x^2)\dot{x}+\gamma x^3 + \omega_0^2 M x\cos(\omega_p t)+A\cos(\omega_e t)\ . \tag{3}$$

The ε factor is introduced in Eq. (2) in order to express, in an explicit form, the degree of nonlinearity of the oscillator.

To obtain analytically the conditions of chaos onset through Melnikov's method, we make use of the fact that at $\delta_0=\delta_1=A=M=0$ the solution is defined by the Hamiltonian [2]

$$H(x,\dot{x})=\frac{y^2}{2}+\frac{\omega_0^2 x^2}{2}-\frac{\varepsilon\gamma x^4}{4}\ . \tag{4}$$

Provided $\gamma>0$, this system possesses two original saddle points in the phase space (x,y), with coordinates

$$y=0\ ,\quad x=\pm\omega_0/\sqrt{\varepsilon\gamma} \tag{5}$$

and a heteroclinic orbit (separatrix) shown in Fig. 1. The solution of the motion equations for $|x|\le\omega_0/\sqrt{\varepsilon\gamma}$ on the separatrix is given by

$$x=x_s(t)=\pm\frac{\omega_0}{\sqrt{\varepsilon\gamma}}\tanh\left[\frac{\omega_0(t-t_0)}{\sqrt{2}}\right],$$

$$y=y_s(t)=\mp\frac{\omega_0^2}{\sqrt{2\varepsilon\gamma}}\left[\tanh^2\left[\frac{\omega_0(t-t_0)}{\sqrt{2}}\right]-1\right],$$

where t_0 is an initial moment of time. The upper and lower signs in these expressions correspond, respectively, to the upper and lower parts of the separatrix in Fig. 1. Note that a coexisting center-type singular point is located at $y=0$, $x=0$ in the phase space of the system (4). The influence of other terms of the function (3) not included in Eq. (4) is considered as a perturbation. Such an approach permits us to apply the standard Melnikov technique developed for similar systems (see Refs. [1–3] for details). We eventually come to the expression defining the formation of the homoclinic structure

$$A\omega_e\operatorname{csch}\left[\frac{\pi\omega_e}{\sqrt{2}\omega_0}\right]+\frac{M\omega_0^2\omega_p^2}{\sqrt{2\varepsilon\gamma}}\operatorname{csch}\left[\frac{\pi\omega_p}{\sqrt{2}\omega_0}\right] \ge\left|\frac{2\omega_0^3}{3\pi\sqrt{\varepsilon\gamma}}\left[\delta_0+\frac{\delta_1\omega_0^2}{5\varepsilon\gamma}\right]\right|. \tag{6}$$

This criterion is usually considered a necessary condition for chaos to arise. It incorporates a variety of particular cases that have been studied so far. For example, assuming $\delta_1=0$, we have from Eq. (6) the condition of a heteroclinic structure arising (obtained in Ref. [2]) for the oscillator with two-frequency excitation. Setting, in addition, $M=0$ in Eq. (6), we arrive at the result given in Ref. [1] for a harmonically forced oscillator.

It is evident from Eq. (6) that chaotic oscillations can arise if there is either only the parametric excitation ($A=0$) or only the external one ($M=0$). Under the combined excitation ($A\neq0$ and $M\neq0$), the threshold of the chaos arising is essentially unchanged.

At first sight this justifies approaches, frequently used for the analysis of stability in parametric amplifiers, when only the pumping signal is taken into account. Such an approach implies that the interaction between the amplified signal and pumping oscillation does not change the stability threshold. However, it will be demonstrated in subsequent sections that there are additional mechanisms leading to chaos at extremely small perturbations, resulting from this interaction.

Now let us consider the transition to the case of a quasilinear oscillator that corresponds to the limit $\varepsilon\to0$. According to Eq. (5), the x coordinate of the saddle points tends to $\pm\infty$ and the value of the Hamiltonian on the separatrix is

$$H_s=\omega_0^4/(4\varepsilon\gamma)\to\infty\ .$$

Suppose that under the influence of perturbation the manifolds of the saddle points intersect transversely, giving rise to a heteroclinic tangle, and a strange attractor appears in the phase space, provided the tangle becomes attractive. Then the maximum values of x on the attractor should also increase as $1/\sqrt{\varepsilon}$ with decreasing ε since the attractor should include one of the saddles. From the motion equation (3) we see that the nonlinear term $\varepsilon\gamma x^3$ tends to infinity as $1/\sqrt{\varepsilon}$. Because of this, the term cannot be considered a small one in such a situation and hence the transition to chaos cannot be considered in the weakly nonlinear limit. However, this observation is true only if we deal with the formation of heteroclinic structures associated with the original saddle points (5). The overall behavior is changed dramatically if we take into account that additional saddle states may arise under the action of external or parametric forces. In this case the interaction of the external frequencies can lead to chaotic states even in the weakly nonlinear limit.

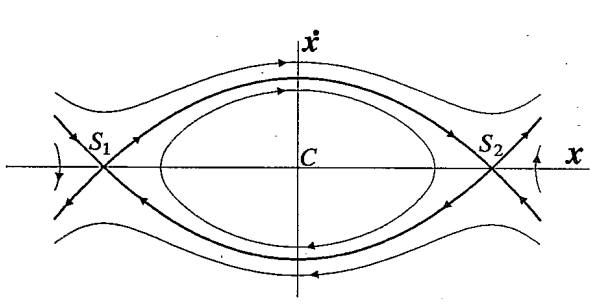

FIG. 1. Phase portrait of the Hamiltonian system (4). S_1 and S_2 are saddle points and C is a center.

III. AVERAGED EQUATIONS

Hereinafter we study the general conditions of chaos arising in weakly nonlinear oscillators, assuming that the right-hand side of Eq. (2) is small, that is, $\varepsilon|f(x,y,t)| \ll 1$. For definiteness, we restrict our consideration by the case of principal parametric resonance when

$$|\omega-\omega_0|=O(\varepsilon\omega_0)\ , \quad |\omega_e-\omega_0|=O(\varepsilon\omega_0)\ , \tag{7}$$

where $\omega \equiv \omega_p/2$. However, it should be stressed that a similar treatment could be given to any other order resonances as well. Then, by using the transformation

$$\begin{aligned} x &= U\cos\omega t + V\sin\omega t\ , \\ y &= -U\omega\sin\omega t + V\omega\cos\omega t\ , \end{aligned} \tag{8}$$

we have instead of (2)

$$\begin{aligned} \dot{U} &= -\frac{\sin\omega t}{\omega}[(\omega^2-\omega_0^2)x+\varepsilon f(x,y,t)]\ , \\ \dot{V} &= \frac{\cos\omega t}{\omega}[(\omega^2-\omega_0^2)x+\varepsilon f(x,y,t)]\ , \end{aligned} \tag{9}$$

where $f(x,y,t)$ and x,y are defined by Eqs. (3) and (8).

The condition of the perturbation smallness and the resonant conditions (7) allow us to apply the method of averaging [30] to these equations. Neglecting the terms $O(\varepsilon^2)$, we have the following system of averaged equations for the slowly varying time functions $U(\tau), V(\tau)$:

$$\begin{aligned} \frac{dU}{d\tau} &= -[\alpha_0+\alpha_1(U^2+V^2)]U \\ &\quad -[\Delta-m+\beta(U^2+V^2)]V-p\sin\Omega\tau\ , \\ \frac{dV}{d\tau} &= -[\alpha_0+\alpha_1(U^2+V^2)]V \\ &\quad +[\Delta+m+\beta(U^2+V^2)]U+p\cos\Omega\tau\ , \end{aligned} \tag{10}$$

where dimensionless parameters are introduced: $\tau=\varepsilon\omega_p t/2$, $\alpha_0=\delta_0/\omega_p$, $\alpha_1=\delta_1/(4\omega_p)$, $m=M/4$, $p=2A/\omega_p^2$, $\beta=3\gamma/(2\omega_p^2)>0$, $\Delta=(\omega_p-2\omega_0)/\varepsilon\omega_p$, and $\Omega=(\omega_p-2\omega_e)/(\varepsilon\omega_p)$.

For mere parametric excitation ($p=0$) this system is reduced to a second-order autonomous system. It is also true for the case of an externally forced oscillator ($m=0$). The latter statement is easily verified with the help of the transformation

$$\begin{aligned} U &= -U^*\cos(\Omega\tau)+V^*\sin(\Omega\tau)\ , \\ V &= -U^*\sin(\Omega\tau)-V^*\cos(\Omega\tau)\ , \end{aligned}$$

which leads to the autonomous system in terms of U^*, V^*.

On this basis we conclude again that weakly nonlinear oscillators with harmonic excitation cannot have any chaotic states. Such states can arise here only due to the interaction of the external frequencies provided that one of the frequency components induces a saddle orbit in the phase space of the system (10).

The transition from the original equations to the averaged ones allows us to reduce the bifurcation problem for two-dimensional tori in the phase space of the original system (1) to the analysis of bifurcations of periodic orbits in the phase space of the system (10). It is important to note that the later system does not contain ε as an independent parameter. The changes in ε lead only to the variation in the time scale of the excited oscillations, provided the values of parameters Δ and Ω are kept constant. From this it follows that, if the system (10) demonstrates chaotic behavior, then such behavior can arise for any degree of ε, however small, i.e, the quasilinear limit.

IV. INDUCED SADDLE STATES

The averaged equations are a convenient tool for the detection of saddle points and the corresponding homoclinic or heteroclinic orbits that arise due to a resonant force. Such saddle states can be induced by both parametric and external forces included in Eqs. (10). We shall consider the case when the amplitude of the external excitation p is relatively small and the induced saddle states can arise mainly due to the parametric component. This case is of prime interest in many practical situations, e.g, for microwave and optical parametric amplifiers where the amplitude of the pumping wave (proportional to m) is much greater than that of the signal wave (proportional to p). The opposite case was considered by Yagasaki [25].

Assuming that the dissipation and the external forcing are absent, we have instead of (10) the Hamiltonian system

$$\begin{aligned} \frac{dU}{d\tau} &= -[\Delta-m+\beta(U^2+V^2)]V\ , \\ \frac{dV}{d\tau} &= [\Delta+m+\beta(U^2+V^2)]U\ , \end{aligned} \tag{11}$$

with Hamiltonian energy given by

$$H(U,V)=-\frac{\beta}{4}(U^2+V^2)^2-\frac{1}{2}[(\Delta-m)V^2+(\Delta+m)U^2]\ . \tag{12}$$

A similar system was investigated in detail in [4] in the context of a period-doubling study in the double-well Duffing equation. For the sake of clarity we will reproduce here some of its basic points. Unlike the previous case [see Eq. (4)], this Hamiltonian contains the amplitude of modulation m as a parameter. In the following we set $m>0$ without loss of generality. As long as $m<\Delta$, there is only a center-type singular point at the origin, whereas for $m>\Delta$ one can find from (11) that the center splits into three (at $m>|\Delta|$) or five (at $m<-\Delta$) singular points. The two possible situations are illustrated by the phase portraits of the system (11) in Fig. 2. Note that the orbits depicted constitute a Poincaré map of the initial system at $\delta_0=\delta_1=A=0$ and at small values of the amplitude of the forced oscillations. When $m>|\Delta|$ (supercritical region), there are three singular points: a saddle point at the origin ($U=0, V=0$) and two centers with coordinates $(U,V)=(0,\pm\sqrt{(m-\Delta)/\beta})$, which are denoted as C_1, C_2 in Fig. 2(a). In the second

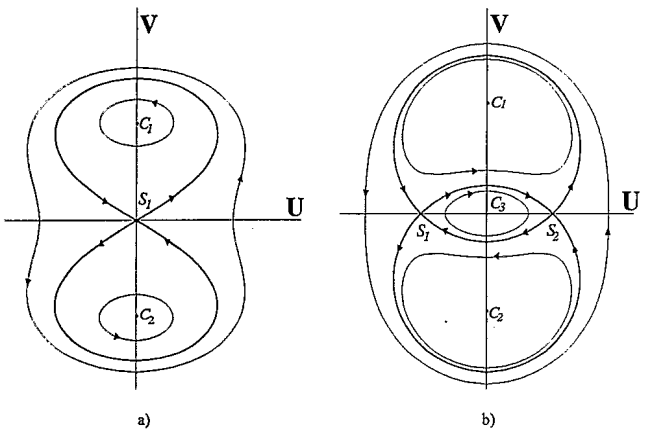

FIG. 2. Phase portraits of the Hamiltonian system (11) for (a) $|\Delta| < m$ and (b) $m < -\Delta$.

case, when $m < -\Delta$ (subcritical region), there are three centers C_1, C_2, C_3 and two saddle points in the phase space with coordinates $U = \mp\sqrt{(-m-\Delta)/\beta}, V = 0$, as shown in Fig. 2(b). Namely because of these saddle points the system possesses induced homoclinic or heteroclinic orbits (separatrices) also indicated in Fig. 2. Because of the induced centers, the system acquires a multistability property when $\alpha_0 \neq 0$ (see below).

Let us now consider in more detail the structure of the separatrix loops for both cases. At $m > |\Delta|$ there is a double symmetric separatrix. The solution of the motion equations (11), $U \equiv U_s(\tau)$ and $V \equiv V_s(\tau)$, on this homoclinic orbit was found in Ref. [16] and can be written in the form

$$U_s(\tau) = \frac{r_1\sqrt{2(m-\Delta)/\beta}\sinh[r_1(\tau-\tau_0)]}{m\cosh[2r_1(\tau-\tau_0)]+\Delta},$$
$$|V_s(\tau)| = \frac{r_1\sqrt{2(m+\Delta)/\beta}\cosh[r_1(\tau-\tau_0)]}{m\cosh[2r_1(\tau-\tau_0)]+\Delta}, \tag{13}$$

where $r_1^2 = m^2 - \Delta^2$ and τ_0 is an initial moment of the "slow" time.

In the second case shown in Fig. 2(b), because of the two saddle points, double heteroclinic orbits arise, to be referred to as small and large orbits. After some calculations one can find the following expression for the solution on these trajectories:

$$U_s(\tau) = \frac{r_2\sqrt{-\Delta/\beta m}\,\sinh[2r_2(\tau-\tau_0)]}{\sqrt{-\Delta}\cosh[2r_2(\tau-\tau_0)]\mp\sqrt{m}},$$
$$|V_s(\tau)| = \mp\frac{-r_2\sqrt{-(m+\Delta)/\beta m}}{\sqrt{-\Delta}\cosh[2r_2(\tau-\tau_0)]\mp\sqrt{m}}, \tag{14}$$

where $r_2^2 = -m(m+\Delta)$ and $\mp$ correspond to the large and small loops of the separatrix, respectively.

Under the influence of dissipation, the areas of the parameter space where the saddle states exist are reduced. However, for any value of the linear ($\alpha_0 < \infty$) and nonlinear ($\alpha_1 < \infty$) dissipation these regions remain finite. Let us analyze this case by introducing the corresponding dissipative terms into the system (11). Then instead of (11), we have

$$\frac{dU}{d\tau} = -[\alpha_0+\alpha_1(U^2+V^2)]U - [\Delta - m + \beta(U^2+V^2)]V,$$
$$\frac{dV}{d\tau} = -[\alpha_0+\alpha_1(U^2+V^2)]V + [\Delta + m + \beta(U^2+V^2)]U. \tag{15}$$

This system yields the following equation for the equilibria:

$$m^2 = (\Delta+\beta W^2)^2 + (\alpha_0+\alpha_1 W^2)^2, \tag{16}$$

where $W^2 = U^2+V^2$ and W is the amplitude of oscillation. Note the existence of a singular point at $W=0$ as well. The amplitudes of stationary states versus Δ (the response curve of the oscillator) are shown in Fig. 3. The saddles are indicated by dashed curves. It is easy to check that the saddle state at $W=0$ exists in the parameter region

$$m > \sqrt{\Delta^2+\alpha_0^2}, \tag{17}$$

whereas if

$$\frac{\beta\alpha_0 - \alpha_1\Delta}{\sqrt{\beta^2+\alpha_1^2}} < m < \sqrt{\Delta^2+\alpha_0^2}, \tag{18}$$

such states are present at $W \neq 0$, provided the frequency detuning Δ satisfies the inequality

$$\Delta < -\frac{\alpha_0\alpha_1}{\beta}. \tag{19}$$

The above given conditions (17)–(19) determine the regions in the parameter space where Melnikov's method can be applied to the system (10). These conditions should be considered as restrictions on the parameters that are complementary to the ones to be found from Melnikov's criterion in subsequent sections. All of them together determine the threshold of chaos arising with

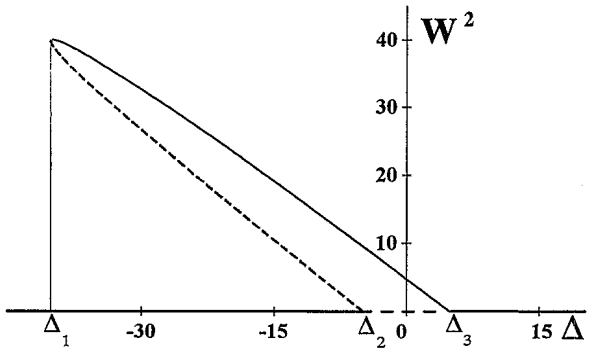

FIG. 3. Response cure of the system (15) for $\alpha_0=1$, $\alpha_1=0.1$, $\beta=1$, and $m=5$. Solid curves correspond to stable states and dashed ones to saddle-type states. The boundaries between regions with different behavior are $\Delta_1 = (\beta\alpha_0 - m\sqrt{\alpha_1^2+\beta^2})/\alpha_1$ and $\Delta_{2,3} = \mp\sqrt{m^2-\alpha_0^2}$.

respect to the amplitude and frequency of the parametric force, thus constituting a resonant condition for chaos to exist.

V. CHAOTIC STATES OF THE OSCILLATOR WITH INDUCED HOMOCLINIC ORBITS

In this section we consider the mechanism of the transition to chaos in the supercritical area, i.e, for the oscillator with the single induced saddle point and a pair of associated homoclinic orbits shown in Fig. 2(a). The second case will be considered in Sec. VI. We start from the application of Melnikov's method to the averaged equations (10) and find necessary conditions for chaos onset with respect to the parameters defining the excitation. Assuming that the dissipation and the amplitude of external force p are small, we write down the Melnikov function $\Delta_M(\tau_0)$, which determines the distance between stable and unstable manifolds of the saddle orbit in the Poincaré cross section of the averaged system

$$\Delta_M(\tau_0)=\int_{-\infty}^{\infty}[R_1(U_s,V_s,\tau)Q_0(U_s,V_s) - Q_1(U_s,V_s,\tau)R_0(U_s,V_s)]d\tau , \quad (20)$$

where

$$R_0=-[\Delta-m+\beta(U_s^2+V_s^2)]V_s ,$$
$$Q_0=[\Delta+m+\beta(U_s^2+V_s^2)]U_s ,$$
$$R_1=-[\alpha_0+\alpha_1(U_s^2+V_s^2)]U_s-p\sin\Omega\tau ,$$
$$Q_1=-[\alpha_0+\alpha_1(U_s^2+V_s^2)]V_s+p\cos\Omega\tau .$$

The functions $U_s(\tau)$ and $V_s(\tau)$ are given by relations (13). After performing the integration in Eq. (20), we find

$$\Delta M(\tau_0)=-\frac{2\alpha_0}{\beta}(r_1-\Delta\theta)+\frac{2\alpha}{\beta^2}[3\Delta r_1-(m^2+2\Delta^2)\theta] + \frac{\pi p\,\Omega\cos(\Omega\tau_0)}{\sqrt{\beta m}\cosh(\pi\sigma_1)}\exp(\theta\sigma_1) , \quad (21)$$

where $\sigma_1=\Omega/(2r_1)$, $\theta=\arccos(\Delta/m)$. The equation defining the manifolds' intersection $\Delta_M(\tau_0)=0$ yields the necessary condition of chaos onset:

$$p\geq\left|\frac{2\sqrt{m/\beta}\cosh(\pi\sigma_1)}{\pi\Omega\exp(\theta\sigma_1)} \times\left\{\alpha_0[r_1-\Delta\theta]-\frac{\alpha_1}{\beta}[3r_1\Delta-(m^2+2\Delta^2)\theta]\right\}\right| . \quad (22)$$

The equality sign corresponds to $p\equiv p_{cr}$, where p_{cr} is the lowest threshold of the homoclinic structure arising with respect to the amplitude of external force. Figure 4 shows a typical dependence of p_{cr} versus Ω for various values of nonlinear dissipation. The function $p_{cr}(\Omega)$ always possesses two minima: one in the region $\Omega>0$ and another at $\Omega<0$. The so-defined threshold of chaos onset has a lower value if $\Omega>0$ and it decreases with the increase of the nonlinearity parameter β and modulation m.

The condition of the manifolds' intersection found from Melnikov's criterion was compared with the threshold of chaos arising from computer experiments. According to current concepts, the manifolds may be expected to touch just before the appearance of a strange attractor in the phase space, which in turn would be the attractive homoclinic structure resulting from the manifolds' intersection.

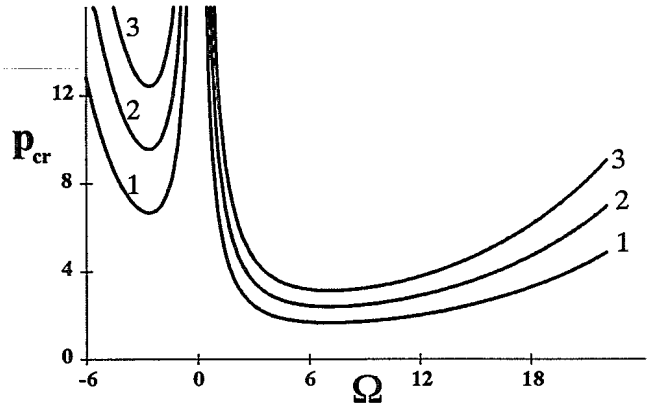

FIG. 4. Threshold of the homoclinc structure arising p_{cr} according to Melnikov's criterion versus Ω for various values of nonlinear dissipation: (1) $\alpha_1=0$, (2) $\alpha_1=0.05$, and (3) $\alpha_1=0.1$ for $\alpha_0=1$, $\beta=1$, $m=5$, and $\Delta=-0.5$.

Prior to discussing the results of numerical experiments, we would like to note that Eqs. (10) are invariant with respect to the transformations $U\rightarrow -U$, $V\rightarrow -V$, and $\tau\rightarrow\tau+\pi/\Omega$. This means that two types of attractors can exist in the phase space of the system: symmetric attractors and/or pairs of asymmetric orbits. Consequently, all bifurcation phenomena observed for one of the asymmetric attractors take place simultaneously for the second one.

An example of the bifurcation diagram obtained in the parameter plane (Ω,p) is shown in Fig. 5. The location of the homoclinic tangency according to the condition (22) is shown by curve 9. The rise of strange attractors found numerically is indicated by curves 6 and 10. One can find reasonably good agreement between these results.

At the same time, there are some evident discrepancies, especially concerning curve 10. In a wide range of Ω variation (approximately $8<\Omega<18$) strange attractors appear before the intersection of manifolds corresponding to the homoclinic trajectories (13) happens. Therefore, the question immediately arises about the origin of the inconsistency between critical values of control parameters from Melnikov's approach and actual ones found by direct numerical integration of the system (10). It could be suggested that the gap between the corresponding curves in Fig. 5 appears because of the approximate character of calculations in the framework of Melnikov's theory, which, being a kind of perturbation analysis, gives an inexact position of the parameter values where the intersection of manifolds occurs. In order to check whether this hypothesis is correct we have computed nu-

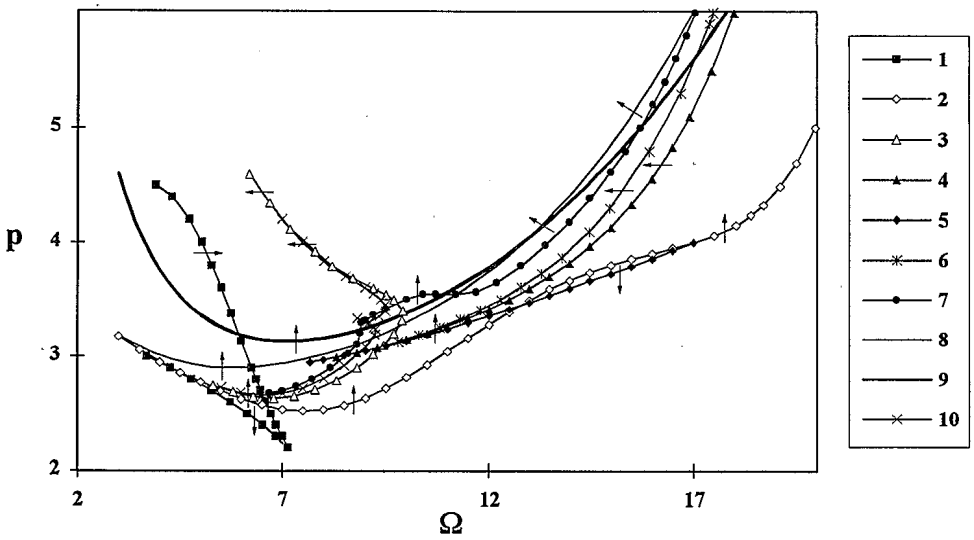

FIG. 5. Bifurcation diagram of the system (10) for $\alpha_0=1$, $\alpha_1=0.1$, $\beta=1$, $\Delta=-0.5$, and $m=5$. Curves 7–9 denote the boundaries of the homoclinic structures formation: 9, according to Melnikov's criterion (22); 8, the same as 9, but found numerically; 7, for the saddle orbit, appearing after the first period-doubling bifurcation (curve 2). Other lines: 1, saddle-node bifurcation in the vicinity of principal external resonance; 3 and 4, second period doubling; 6 and 10, boundaries of strange attractors arising near the principal parametric and external resonances, respectively. Arrows indicate the direction of change in the control parameters where the bifurcations described in the text occurs. For lines 1 and 5 arrows show the way for jumps between different coexisting attractors.

merically the invariant manifolds of the periodic saddle orbit in a Poincaré cross section of the phase space. The actual boundary in the parameter plane, where the stable and unstable manifolds corresponding to the homoclinic trajectories (13) [see also Fig. 2(a)] touch, is denoted by the curve 8 in Fig. 5. It is thus clear that the above conjecture is wrong and hence some other mechanisms of chaotic attractors formation, different form the one amenable to Melnikov's method, should be considered. It is also evident from Fig. 6, where the plot of a typical structure of the intersected manifolds on the Poincaré plane together with two coexisting chaotic attractors is shown. Note that the strange attractors, although located very close to the homoclinic structure, do not coincide with the outset of the saddle.

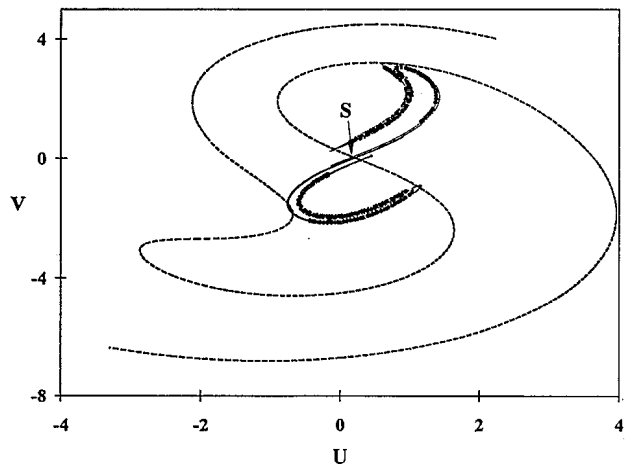

FIG. 6. Poincaré map of the system (10) with stable (dashed curves) and unstable (solid curves) manifold associated with the induced homoclinic orbit (13) for $p=5.5$, $\Omega=16$, $\alpha_0=1$, $\alpha_1=0.1$, $\beta=1$, $\Delta=-0.5$, and $m=5$. Dots indicate the position of two strange attractors on the Poincaré plane.

To gain a better insight into the mechanism of the appearance of chaos, let us trace some characteristic bifurcations in the system. It should be noted here that Eqs. (10) describe the motion in an oscillatory system. Therefore, the system should possess resonant properties that play important role in the dynamics. Within the parameter range considered we have detected two resonant areas with different chaotic attractors in each of them. They correspond, respectively, to the principal resonance ($\Omega\approx\Omega_0$) in the vicinity of foci (centers C_1, C_2 after introducing the dissipation) and the main parametric resonance ($\Omega\approx 2\Omega_0$), where Ω_0 stands for the natural frequency of the oscillations at $p=0$.

Interesting enough is that the properties of averaged equations (10) describing the dynamics of system (1) under two frequency excitation are qualitatively analogous to those of Eq. (1) at harmonic excitation [4,31,32] (see also, Sec. IV). Indeed, for example, at $\Omega=\Omega_{1/2}\approx 17$, $p=p_{1/2}\approx 4$ one can easily recognize the organizing center for the principal parametric resonance, corresponding to the border between the sub- and the super criticality of a period-doubling bifurcation. In the vicinity of this point the qualitative picture of dynamics corresponds to the one following from expressions (18) and (19) for the system (15). We thus see in a sense the self-similarity of the oscillator (1) under the specific type of excitation considered in the present work. At $\Omega=\Omega_1\approx 7.2$, $p=p_1\approx 2.2$ the principal external resonance occurs manifesting itself in well-known hysteretic jumps between attractors resulting from the saddle-node bifurcation, when crossing the border of the area delineated by curve 1 on Fig. 5.

For the sake of clarity we consider now what happens if p is increased while the value of $\Omega>\Omega_1$ is kept constant for the both resonances shown in Fig. 5. The case $\Omega<\Omega_1$

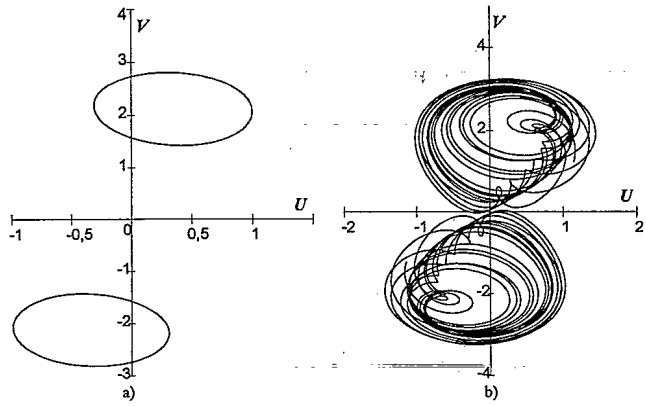

Fig. 7. Two coexisting (a) regular attractors for $p=2.5$ and $\Omega=13$ and (b) chaotic attractors for $p=4$ and $\Omega=13$.

will be described in detail in Sec. VI in the context of heteroclinic saddle points. At small p we observe two stable periodic orbits (two coexisting symmetric attractors) as shown in Fig. 7(a), which arise in the vicinity of former centers C_1, C_2 existing in the Hamiltonian system (11). At lines 2 or 5 the attractors undergo the first period-doubling bifurcation. Then one can observe a few further periodic doublings resulting in different chaotic attractors for both resonances. A pair of strange attractors arises at each of the lines 6 or 10, corresponding to parametric and external resonances, respectively, as illustrated in Fig. 7(b) for the former case. Our analysis has shown that for both resonances the homoclinic structure originating from additional saddle orbits, which typically arises after each of period doublings in the place of losing their stability periodic motions, plays the key role in the formation of chaos. The structure of stable and unstable manifolds of such an additional saddle period-1 orbit in the Poincaré section is depicted in Fig. 8, along with the

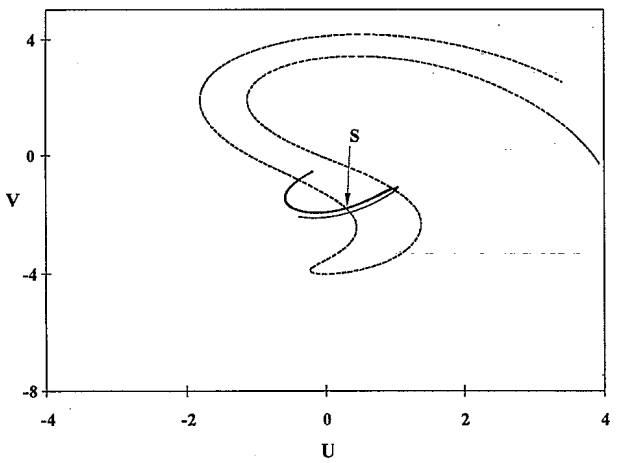

FIG. 8. Poincaré map of the system (10) with stable (dashed curves) and unstable (solid curves) manifolds associated with the saddle orbit S arising after the first period-doubling bifurcation for $p=5.5$, $\Omega=16$, $\alpha_0=1$, $\alpha_1=0.1$, $\beta=1$, $\Delta=-0.5$, and $m=5$.

coordinates of the saddle. The touching of the manifolds occurs at curve 7 in Fig. 5. This curve fits the borders 6 and 10 a little better than 8. A comparison of Figs. 6 and 8 demonstrates that it is the outset of the saddle shown in Fig. 8 that coincides with the chaotic attractor shown in Fig. 6. Our experiments also indicate that just after the accumulation point of period doublings, i.e., after the strange attractor arises at line 6 or 10, the intersection of manifolds of high-period unstable orbits occurs, being presumably the main reason for chaos to arise.

The given example of the bifurcation diagram shows again that the application of Melnikov's technique should always be accompanied by additional detailed numerical experiments because of a variety of possible roads to chaos. Additional examples in favor of this point will be given in the next section.

VI. CHAOTIC STATES OF THE OSCILLATOR WITH INDUCED HETEROCLINIC ORBITS

In this section we shall analyze the conditions for the chaos onset and study some properties of the system (10) for the case $|\Delta|>m$. We being again from Melnikov's criterion. To derive it explicitly, we can use again the expressions (20) for the distance between stable and unstable manifolds $\Delta_M(\tau_0)$ in Poincasé map. For the case under consideration, the functions $U_s(\tau)$ and $V_s(\tau)$ involved in (20) are given by the expressions (14). Performing the integration in (20), we have

$$\Delta_M(\tau_0)=\frac{2\alpha_0}{\beta}[r_2\mp\Delta\theta^{\mp}]-\frac{2\alpha_1\Delta}{\beta^2}[3r_2\pm(2m-\Delta)\theta^{\mp}] + \frac{2\pi\sigma_2 p\sqrt{-(m+\Delta)/\beta}\cos(\Omega\tau_0)}{\sinh(\pi\sigma_2)} \times\exp(\pm\sigma_2\theta^{\mp}), \tag{23}$$

where $\sigma_2=\Omega/(2r_2)$ and $\theta^{\mp}=\arccos(\mp\sqrt{-m/\Delta})$. The upper and lower signs correspond to the large and small separatrix loops [see Fig. 2(b)], respectively. Setting $\Delta_M(\tau_0)=0$, we get from (23) the condition of the manifolds intersection

$$p\geq\left|\frac{\sinh(\pi\sigma_2)}{\pi\sigma_2\sqrt{-(m+\Delta)/\beta}\exp(\pm\sigma_2\theta^{\mp})} \times\left\{\frac{\alpha_0}{\beta}[r_2\mp\Delta\theta^{\mp}]-\frac{\alpha_1\Delta}{\beta^2}[3r_2\pm(2m-\Delta)\theta^{\mp}]\right\}\right|. \tag{24}$$

A typical example of the bifurcation diagram in the parameter plane (p,Ω) obtained numerically, together with Melnikov's criterion (curve 1), is given in Fig. 9. It should be stressed that the overall bifurcation pattern shown in Fig. 9 in many respects similar to the one given in Fig. 5. The only essential difference consists in the part concerning the attractor in the vicinity of origin, which is, of course, absent in the case considered in Sec. V. The best way to explain all possible types of behavior in the system is again to start from the Hamiltonian case,

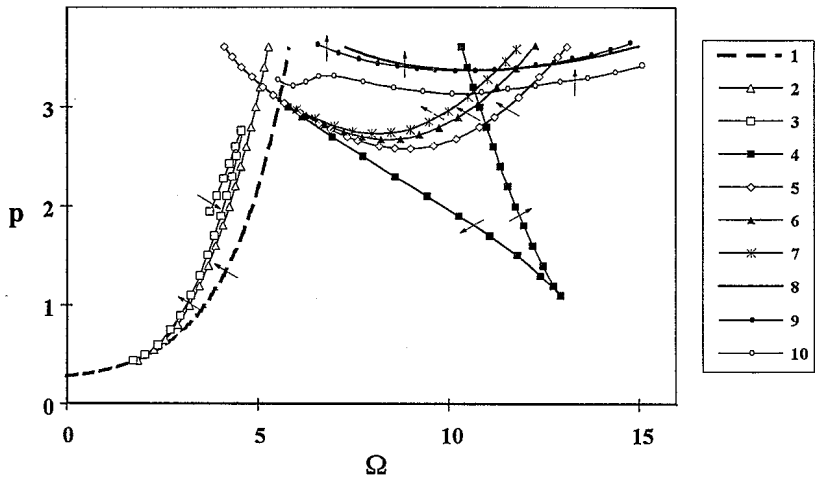

FIG. 9. Bifurcation diagram of the system (10) at $\alpha_0=1$, $\alpha_1=0$, $\beta=1$, $\Delta=-6$, and $m=5$. Curves 1–3 correspond to the attractors formed on the base of the small heteroclinic loop: 1, the boundary of the existence of homoclinic structure according to Melnikov's criterion; 2, symmetry breaking; 3, the first period-doubling bifurcation. Curves 4–7 are related to the attractors due to the principal external resonance: 4, saddle-node bifurcation; 5 and 6, first and second periodic-doubling bifurcations; 7, attractor crises. Curves 9 and 8 correspond to the large heteroclinic loop and represent boundaries of the existence of homoclinic structure found numerically and with Melnikov's criterion correspondingly. Curve 10 denotes the position where the intersection between the stable manifold of the small loop and the unstable manifold of the large loop takes place.

i.e., Fig. 2(b), and then set $\alpha_0 \neq 0$. Thus, we obtain three stable foci instead of three centers and all trajectories will eventually go to one of them, depending on initial conditions. We mark the attractors that arise in the vicinity of centers C_1, C_2, C_3 as A_1, A_2, A_3, respectively, that is, the system is three-stable initially. Provided the amplitude p is small enough, the foci turn to stable periodic orbits and the three of them exist simultaneously in the phase space. The attractor A_3 undergoes the symmetry breaking crises (pitchfork bifurcation) at curve 2, and to the left of it, four attractors (A_1, A_2, A_3, A_3') coexist in the phase space. At curve 3 both attractors A_3, A_3' undergo the first period-doubling bifurcation and then a pair of strange attractors appears through the period-doubling cascade. In Fig. 10(a) the situation is given when these two attractors merge and a unified strange attractor aries. It turns out that the strange attractors in this parameter region are very sensitive to the variation of parameters and exist only in a very narrow band adjacent to curve 3. Obviously, their basins of attraction are small and the majority of initial conditions lead to two stable attractors coexisting with them.

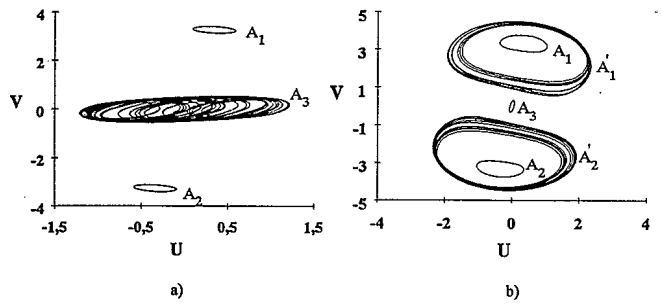

FIG. 10. All coexisting attractors of the system (10) at (a) $\Omega=3.95$ and $p=1.9$ and (b) $\Omega=9.2$ and $p=2.8$ for $\alpha_0=1$, $\alpha_1=0$, $\beta=1$, $\Delta=-6$, and $m=5$.

In this area of the parameter plane the rise of strange attractors may be associated with the intersection of manifolds originating from the small loop. Hence, in this case Melnikov's criterion seems to work well and good predictions can be developed on its basis.

Another region of chaos in Fig. 9, with much higher values of the threshold in the amplitude p, is related to the principal external resonance in the system (10). Let us trace the bifurcations leading to the chaos arising with the increase in the amplitude p at fixed $\Omega=9.2$. If p is small, then there are also three coexisting periodic attractors A_1, A_2, A_3. At $p \geq 1.1$ within the parameter area delimited by curve 4 in Fig. 9 each of the orbits A_1 and A_2 splits into two stable (A_1, A_1' and A_2, A_2') and one saddle (A_1'' and A_2'') orbits. This happens because of the tangent (or saddle-node) bifurcation under the influence of the external force. Note that in this parameter region the period-1 saddle orbits induced by the parametric and additive forces coexist. With the p value increasing, the stable orbits A_1' and A_2' transform to strange attrators through period doublings, starting from line 5. In this area the chaotic dynamics is strongly influenced by the homoclinic structure due to the intersection of stable and unstable manifolds of the saddle orbits A_1'' and A_2'' induced by the external force. Initially, two strange attractors may coexist with three regular ones, as is shown in Fig. 10(b). The extreme sensitivity of these strange attractors to small fluctuations also takes place in this case. The chaotic oscillations exist only in a narrow area near period doublings between curves 6 and 7 and any phase trajectory is eventually attracted to periodic orbits after chaos breaks down.

As in Sec. V, Melnikov's technique does not allow us to predict the appearance of these strange attractors. The intersection of manifolds originating from the large loop

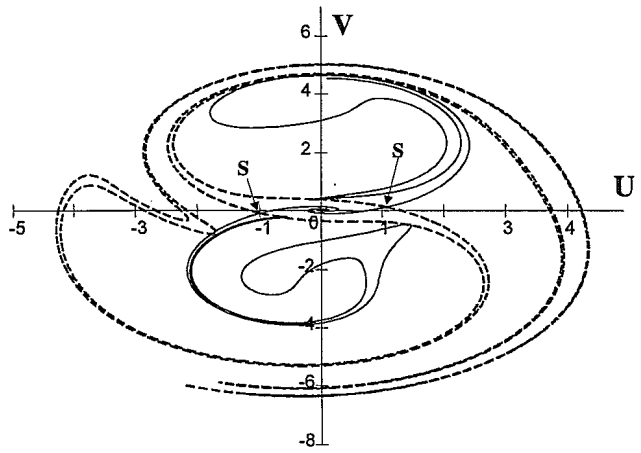

FIG. 11. Intersection of the stable (dashed curve) manifold of the small loop and the unstable (solid curve) manifold of the large loop in the Poincaré section for $p=3.2$, $\Omega=12$, $\alpha_0=1$, $\alpha_1=0$, $\beta=1$, $\Delta=-6$, and $m=5$.

associated with the parametrically induced saddles $S_{1,2}$ [see Fig. 2(b)] takes place at relatively large values of the external amplitude indicated by curve 8 in Fig. 9. This curve practically coincides with that found from Melnikov's criterion (curve 9). One can conclude again that the method is rather accurate in predicting the appearance of a homoclinic structure but cannot be used as an exact predictor of chaotic dynamics. On the other hand, a better result could probably be obtained through Melnikov's method by considering the parametric force as a perturbation rather than the external force (see, e.g., Ref. [25]).

At the same time, another peculiarity has been found next to curve 10, where a specific type of homoclinic structure formation has been observed. In this region an additional homoclinic structure is formed, resulting from the intersection of the manifolds from different loops, large and small, but not from either one of them alone. This situation is illustrated in Fig. 11, where the crossing of the unstable manifold of the large loop and the stable manifold of the small loop takes place. We thus observe two different mechanisms for the same manifolds: either the heteroclinic tangency and crossing at line 8 or the homoclinic intersection at curve 10. Such a mechanism has not received much attention and has practically not been studied yet. It seems interesting to find other systems exhibiting this road to complicated behavior, as well as to develop an analytical tool to detect the presence of such homoclinic structures.

VII. DISCUSSION AND CONCLUSIONS

In this paper, we have considered the conditions of the chaotic states arising in weakly nonlinear Duffing-type oscillators subjected to the combined parametric and external forcing. It was shown that the homoclinic or heteroclinic orbits induced by one of the external harmonic components play a crucial role in the oscillator dynamics. Because of these orbits, the formation of a homoclinic (or heteroclinic) structure takes place in the weakly nonlinear limit under the action of incommensurate frequencies and the chaos onset occurs due to the destruction of a two-dimensional torus. The generality of these results does not depend on the type of perturbation considered and they most probably hold for a variety of single-degree-of-freedom systems with quasiperiodic force.

Chaotic states of weakly nonlinear oscillators manifest themselves in the form of a weak chaotic modulation of the amplitude and phase of the periodic oscillation with the frequency close to the natural one ω_0 of the oscillator. The characteristic time scale of the modulation is of the order of ω_0/ε, which is much greater than $1/\omega_0$. As a result, the direct investigation of these states by using the governing equation of type (1) for the oscillator dynamics would lead to a cumbersome computational procedure. There are also no analytical methods that could detect the chaotic states in this case. One way to avoid these problems is to use the averaging method. The averaged equations essentially simplify the computational problems, but, more importantly, they provide a great field for the application of analytical methods for chaos detection. In this way we have determined the conditions for the formation of chaotic states on the basis of homoclinic and heteroclinic orbits induced by the parametric forcing. These analytical results include, in the first place, the arising conditions (17)–(19) for the induced saddle states, which give the critical values of the parametric force amplitude and frequency range where chaos may arise. A complementary condition of the parameters defining the external force have been obtained in the framework of Melnikov's technique and is given by Eq. (22) or (24). Joint application of above-mentioned criteria enables us to define quite accurately the regions in the control parameter space where chaos may arise in the weakly nonlinear limit.

It should be noted that these conditions, unlike those obtained for the strongly nonlinear oscillator, do not contain explicitly the parameter ε, as well as the equations of the induced separatrix loops. Because of this property, the restriction imposed by the perturbation smallness $\varepsilon|f(x,y,t)| \ll 1$ is no longer in contradiction with the conditions of the chaos onset and hence the chaotic states can arise in physical systems with any degree of nonlinearity, however small. Variation in the ε value leads only to a change in the characteristic time scale of the chaotic modulation.

We detailed some of the phenomena that accompany the chaos onset. Multistability of the oscillator conditioned by the formation of several attracting sets in the phase space is one of them. This study, along with the foregoing ones [6,18,31,32], suggests that the multistability is a typical feature of the forced nonlinear oscillators. It has been shown in this paper that the splitting of a center-type singular point into several stable and unstable orbits under the action of the resonant periodic force is primarily responsible for the multistability property of the oscillator, at least for relatively small values of the

force amplitude.

Three typical mechanisms leading to complicated behavior in the system under investigation, depending upon the manner of the homoclinic (heteroclinic) structure formation have been discussed. Let us cite them as they appeared, in terms of the averaged equations. The first one is through the intersection of stable and unstable manifolds of some parametrically or externally induced homoclinic or heteroclinic loop (see Fig. 6). The second one is through the manifolds' intersections of additional saddle orbits resulting from the loss of stability of stable periodic motions in period doubling bifurcations (see Fig. 8). The third road is through the intersection of stable and unstable manifolds associated with different loops (see Fig. 11).

An important motivation for this work results from experimental investigations of microwave parametric amplifiers, which clearly indicated that the amplifiers, stable under the action of only pumping oscillation or signal wave, lose their stability when both oscillations are applied simultaneously [26]. The results of this paper give an explanation of such a phenomenon and provide mathematical tools for its study and prediction. It is also obvious that our results are applicable, within certain limits, to other types of similar devices, say, Josephson-junction parametric amplifiers and optical amplifiers. It is worth noting that the factors that are responsible for the chaos onset in the weakly nonlinear limit and hence for the low stability threshold of the parametric amplifiers are precisely the same as the ones that provide the low noise amplification property from the point of view of the conventional theory of parametric devices. Indeed, according to the classical results of this theory, parametric amplifiers possess a low noise output level because they consist of a reactive circuit (nonharmonic oscillator) and they utilize an ac power supply (pumping oscillation). In terms of the mathematical model used in this paper, the reactive type of nonlinearity is described by the component with parameter γ and the pumping amplitude is given by the parameter m [see (1)]. Proceeding from the results obtained, it is clear that exactly the combination of this type of nonlinearity and the form of parametric excitation lead to the possibility of the chaos onset in the weakly nonlinear limit, when the external signal is applied. Thus this seems to be the main reason why the parametric amplifiers, along with a number of similar practical systems, are extremely susceptible to chaotic instabilities.

ACKNOWLEDGMENTS

This research was supported by the International Science Foundation (Grant No. U33000). V.B.R. acknowledges support from the Science and Technology Agency of Japan.

[1] V. K. Melnikov, Trans. Moscow Math. Soc. No. 12, 3 (1963).
[2] A. D. Morosov, Diff. Equations No. 12, 164 (1976).
[3] P. Holmes, Philos. Trans. R. Soc. London Ser. A **292**, 419 (1979).
[4] C. Holmes and P. Holmes, J. Sound Vib. **78**, 161 (1981).
[5] V. B. Ryabov and H. M. Ito (unpublished).
[6] Y. Ueda, S. Yoshida, H. B. Stewart, and J. M. T. Thompson, Philos. Trans. R. Soc. London Ser. A **332**, 169 (1990).
[7] J. M. Guckenheimer and P. Holmes, *Nonlinear Oscillations, Dynamical Systems and Bifurcations of Vector Fields* (Springer, Berlin, 1983).
[8] K. Ide and S. Wiggins, Physica D **34**, 169 (1989).
[9] S. Wiggins, Phys. Lett. A **124**, 138 (1987).
[10] J. Miles, Appl. Phys. Math. Sci. **81**, 3919 (1984).
[11] A.B. Belogortsev, D. M. Vavriv, and O. A. Tret'yakov, Zh. Eksp. Teor. Fiz. **92**, 1316 (1987) [Sov. Phys. JETP **65**, 737 (1987)].
[12] K. Yagasaki, M. Sakata, and K. Kimura, ASME J. Appl. Mech. **57**, 209 (1990).
[13] A. B. Belogortsev, D. M. Vavriv, and B. A. Kalugin, Zh. Tekh. Fiz. **57**, 559 (1987) [Sov. Phys. Tech. Phys. **32**, 337 (1987)].
[14] I. Yu. Chernyshov and D. M. Vavriv, in *Proceedings of the International Conference on Noise in Physical Systems,* edited by A. Ambrozy (Akademiai Kiado, Budapest, 1990), p. 651.
[15] A. B. Belogortsev, D. M. Vavriv, and O. A. Tret'yakov, Zh. Tekh. Fiz. **58**, 284 (1988) [Sov. Phys. Tech. Phys. **33**, 174 (1988)].
[16] D. M. Vavriv, V. B. Ryabov, and I. Yu. Chernyshov, Zh. Tekh. Fiz. **61**, 1 (1991) [Sov. Phys. Tech. Phys. **36**, 1325 (1991)].
[17] S. A. Bulgakov, V. B. Ryabov, V. I. Shnyrkov, and D. M. Vavriv, J. Low Temp. Phys. **83**, 241 (1991).
[18] A. C. Skeldon and T. Mullin, Phys. Lett. A **166**, 224 (1992).
[19] A. B. Belogortsev, D. M. Vavriv, and O. A. Tret'yakov, Izv. Vyssh. Uchebn. Zaved. Radiofiz. **33**, 238 (1990) [Radiophys. Quantum Electron. **33**, 187 (1990)].
[20] A. B. Belogortsev, D. M. Vavriv, and O. A. Tret'yakov, Zh. Tekh. Fiz. **61**, 15 (1991) [Sov. Phys. Tech. Phys. **36**, 389 (1991)].
[21] D. M. Vavriv and O. A. Tret'yakov, *Theory of Resonant Amplifiers with Distributed Interaction of O-type* (Naukova Dumka, Kiev, 1987).
[22] K. Wiesenfeld and B. McNamara, Phys. Rev. A **33**, 629 (1986).
[23] S. T. Vohra, L. Fabini, and K. Wiesenfeld, Phys. Rev. Lett. **72**, 1333 (1994).
[24] M. S. Soliman and J. M. T. Thompson, Proc. R. Soc. London Ser. A **438**, 511 (1992).
[25] K. Yagasaki, ASME J. Appl. Mech. **58**, 244 (1991).
[26] I. Yu. Chernyshov and D. M. Vavriv, Phys. Lett. A **165**, 117 (1992).
[27] B. Ravindra and A. K. Malik, Phys. Rev. E **49**, 4950 (1994).
[28] W. Szemplinska-Stupnicka and J. Rudowski, Physica D **66**, 368 (1993).
[29] L. D. Zavodney, A. H. Nayfeh, and N. E. Sanchez, J.

Sound Vib. **129**, 417 (1989).

[30] N. N. Bogoliubov and Yu. A. Mitroposki, *Asymptotic Methods in the Theory of Nonlinear Oscillations* (Gordon and Breach, New York, 1961).

[31] V. B. Ryabov and D. M. Vavriv, Phys. Lett. A **153**, 431 (1991).

[32] D. M. Vavriv and V. B. Ryabov, Pis'ma Zh. Tekh. Fiz. **17**, 55 (1991).